Wisconsin Electric POWER COMPANY
231 W. MICHIGAN, P.O. BOX 2046, MILWAUKEE, WI 53201

August 28, 1979

Mr. J. G. Keppler, Director
Office of Inspection and Enforcement
Region III
U. S. NUCLEAR REGULATORY COMMISSION
799 Roosevelt Road
Glen Ellyn, Illinois 60137

Dear Mr. Keppler:

DOCKET NOS. 50-266 AND 50-301
FURTHER RESPONSE TO IE BULLETIN 79-13
POINT BEACH NUCLEAR PLANT, UNITS 1 AND 2

On June 25, 1979, the Office of Inspection and Enforcement issued IE Bulletin 79-13 which required PWR licensees to inspect at least a portion of steam generator feedwater piping systems and to report the results of these inspections to NRC. Our submittal of July 12, 1979 fulfilled the bulletin requirements for Point Beach Nuclear Plant Unit 2 and presented our initial plan for the Unit 1 inspections.

The final metallurgical evaluation report for the Unit 2 feedwater pipe reducer is provided in the enclosure to this letter. In addition, during our review of this subject, we have revised the listing of transients and the piping stress isometrics from that initially provided with our July 12 submittal. This revised information is also contained in the enclosure.

The metallurgical evaluation of the Unit 2 steam generator reducer identifies the deepest crack as less than 0.047 inches into the pipe wall. The cracks were circumferentially oriented and no microstructural dependence was observed. These minor cracks have apparently been present for some considerable length of time based upon the chemistry analysis of the deposited oxides. The report concludes that the most probable cause of this cracking is corrosion fatigue. As discussed in the enclosure, and in our previous submittal, we consider that the existence of these cracks does not present an unsafe condition for continued plant operation.

During the Unit 1 refueling scheduled to begin September 28, 1979, we intend to replace the Unit 1 main feedwater piping from the steam generator nozzle back to the main check valve. Also, we intend to inspect, and repair as necessary, the auxiliary feedwater piping to a minimum of three feet upstream of the connection to the main feedwater piping.

The design of the Point Beach steam generators utilizes a common feedwater inlet nozzle for the injection of both normal and auxiliary feedwater. As indicated on the stress isometrics, the auxiliary feedwater connection to the main feedwater piping is close to the steam generator nozzle and is downstream of the main feedwater check valve. Up to this point, water supply to the steam generators is provided by separate piping systems. A thermal evaluation of the auxiliary feedwater piping, which is contained in the enclosure, has conservatively shown that only three feet of auxiliary feedwater pipe closest to the main feedwater pipe experiences a significant thermal transient. Beyond this distance, there is no reasonable thermal fatigue mechanism present. As you are aware, the preliminary conclusion concerning the development of these cracks is that it is corrosion assisted fatigue and that the cyclic stress caused by thermal transients may be the prime cause. Therefore, by assuring the integrity of the main feedwater piping downstream of the check valve and the auxiliary feedwater piping that is subject to thermal transients, the water supply to the steam generators is assured. Our repair program responds to the bulletin in assuring the integrity of feedwater supply to the steam generators. Accordingly, the remaining welds inside containment in the main feedwater system will not be inspected as the existence of small cracks in these welds is of no significance.

The Unit 1 main feedwater piping that will be replaced, will also be removed from inside containment and inspected at a later time. We consider it highly probable that minor indications, such as those found on Unit 2, will be found during the Unit 1 inspections. We will provide a report of the results of the inspection after completion of the refueling outage.

Should you have questions, we would be pleased to discuss this program further.

Very truly yours,

C. W. Fay, Director
Nuclear Power Department

Enclosure

Copy to: Office of Inspection and Enforcement
Division of Reactor Operations Inspection

Mr. A. Schwencer, Chief
Office of Nuclear Reactor Regulation

ENCLOSURE

RESPONSE TO
IE BULLETIN 79-13
AUGUST 28, 1979

This enclosure discusses and provides the following items for the Point Beach Nuclear Plant with respect to the subject bulletin:

a. Revised main feedwater piping stress isometrics for both nuclear units; these supersede the figures contained in Wisconsin Electric's July 12 submittal to NRC.

b. Revised tables of Significant Operating Events for Feedwater Piping System Transients; these supersede the tables contained in Wisconsin Electric's July 12 submittal to NRC.

c. The results of a thermal transient analysis of the Point Beach Nuclear Plant auxiliary feedwater piping by Bechtel Power Corporation

d. A copy of Appendix B of the Southwest Research Institute Report, "Point Beach Nuclear Plant, Unit 2 Feedwater and Auxiliary Feedwater System Examination, Analysis, and Repair"; SwRI Project 17-4048, August 1979.

A. PIPING STRESS ISOMETRICS

Figures 1 thru 4 attached present a summary of stresses, based upon the original analyses, of the four Point Beach Nuclear Plant main feedwater pipes. The stresses are presented for piping beyond that inspected on Unit 2 or to be inspected on Unit 1. The Unit 1 program will encompass welds analogous to the welds inspected on Unit 2 (which are denoted on the Unit 2 figures).

The original piping analysis was performed to satisfy the B31.1 design requirements. Because the piping gravity supports were designed independently of the seismic supports, a conservatively assumed gravity stress of 3000 psi was used in the stress combinations. To check the validity of this assumption, a gravity stress analysis was recently performed for the Unit 1 "B" piping loop. The highest calculated gravity stress was 647 psi at the data point representing the piping connection to the containment penetration (not shown on the attached figure). A comparison of the other calculated gravity stresses for the Unit 1 "B" loop to the assumed gravity stress utilized on the other three piping loops shows a substantial degree of conservatism in this assumption. Also, as discussed in our July 12 submittal, the original analysis assumed all 16-inch diameter piping; the larger 18 inch diameter reducer-to-nozzle joint section modulus was not considered. Thus, the stresses for data point 5 on the attached figures are again conservative.

1044 237

The stress results from the computer analysis of the entire main feedwater piping inside containment have been reviewed for all four pipelines. A comparison of the total SSE stress results (which includes gravity and longitudinal pressure stresses) to an allowable stress of 27,000 psi (1.8 S_h, which is lower than the material yield strength) indicates the following:

1. All total SSE stresses are less than 80% of allowable.

2. About 65% of the data points in all four loops have total SSE stresses less than 40% of allowable.

B. TABLES OF SIGNIFICANT OPERATING EVENTS

The attached Tables 1 and 2 replace Tables 2 and 3 of our July 12 submittal to NRC. These tables have been revised to further identify and clarify significant thermal transients experienced by the main feedwater piping. The normal feedwater temperatures (No. 5 feedwater heater outlet) are as follows (100% power = 497 MWe net):

Power Level, %	Approximate Feedwater Temp., °F
100	435
95	427
78	405
52	371
26	323
0	70 to 100

The zero percent power level represents a hot shutdown condition. In this situation, feedwater may be supplied from different sources. The source of feedwater is selected by the plant operators dependent upon why the plant is in the hot shutdown condition. The attached tables do not include events occurring at, or close to, the 0% power level since these events are not considered to cause significant thermal transients in the feedwater system.

C. AUXILIARY FEEDWATER PIPING THERMAL EVALUATION

The attached thermal evaluation of the auxiliary feedwater piping was performed by Bechtel Power Corporation and presents the temperature profile during normal steady-state plant conditions. The analysis conservatively shows that the temperature in the auxiliary feedwater piping wall decreases to 150°F within a distance of 3 ft; the 3 feet is rounded off from the 1 foot mixing zone plus 1.5 feet from analysis. This delta T (270°F) magnitude would decrease if the steady-state main feedwater temperature decreased.

Assuming that the minimum auxiliary feedwater temperature is 32°F (service water is a potential source of supply), the maximum temperature differential in the piping upstream of this 3-foot point, in practical terms, would be less than 115F°. In Timoshenko, "Strength of Materials", Part II, Third Edition, Section 27 discusses thermal stresses in cylindrical shells. Utilizing reasonable carbon steel properties, a temperature

difference of 115 F° would be calculated to produce a maximum bending stress (thermal) of about 15,000 psi. Thus, it is concluded that the only portion of the auxiliary feedwater piping that is exposed to a significant thermal transient is the approximately 3 feet of pipe closest to the main feedwater pipe. During the Unit 1 refueling outage, at least this section of the auxiliary feedwater pipe will be inspected and/or replaced as deemed appropriate.

D. FINAL METALLURGICAL EVALUATION REPORT

The laboratory metallurgical evaluation of the Unit 2 "A" reducer was performed by the Southwest Research Institute (SwRI) of San Antonio, Texas. The final report by SwRI containing the inspection results, procedures used, procedure qualification records, certifications, etc., is available at the Point Beach Nuclear Plant.

Appendix B (33 pages) attached hereto entitled, "Metallurgical Evaluation of Feedwater Pipe Cracking" is the pertinent section of this SwRI report. This appendix supersedes the preliminary information contained in our July 12 submittal to NRC. Conclusions from the report are:

- the most probable cause of cracking is corrosion fatigue.
- the deepest penetration found was less than 0.047 inches
- the cracks appear to have been present for some time based upon chemistry analysis of the oxides. Crack tips are invariably blunt and oxide filled.
- the cracks were invariably circumferentially oriented (absence in the axial direction) and no microstructural dependence was observed.
- the toughness of the reducer material at temperatures above 100°F and the ductility of carbon steel renders a catastrophic failure improbable.

These conclusions are basically the same as those presented in the preliminary report.

CALCULATION SHEET

SHEET OF

FILE No.

SUBJECT BEACH NUCLEAR PLANT MADE BY DATE

MAIN FEEDWATER - Unit 1, "A" CHKD. BY DATE

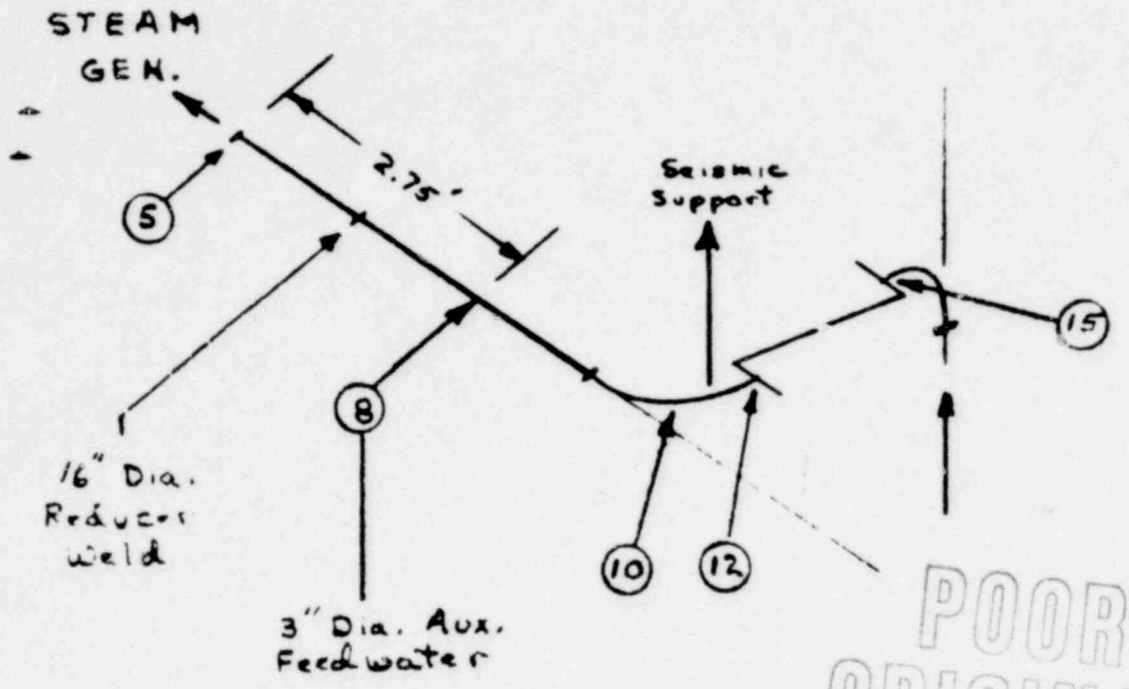

STRESS SUMMARY

Data Point	Thermal Stress, psi	Gravity Stress, psi	Longitudinal Pressure stress, psi	Total Seismic Stress, psi OBE	SSE	REMARKS
5	3021	3000	3608	12532	18456	Nozzle
8	3728*	3000	3608	9546*	12484*	Aux. F-W Connec.
10	5700	3000	3608	13331	20054	Elbow
12	455	3000	3608	8546	10484	End Bend
15	6043	3000	3608	8289	9970	Begin Bend

*Stress intensification factor not included.

FIGURE 1

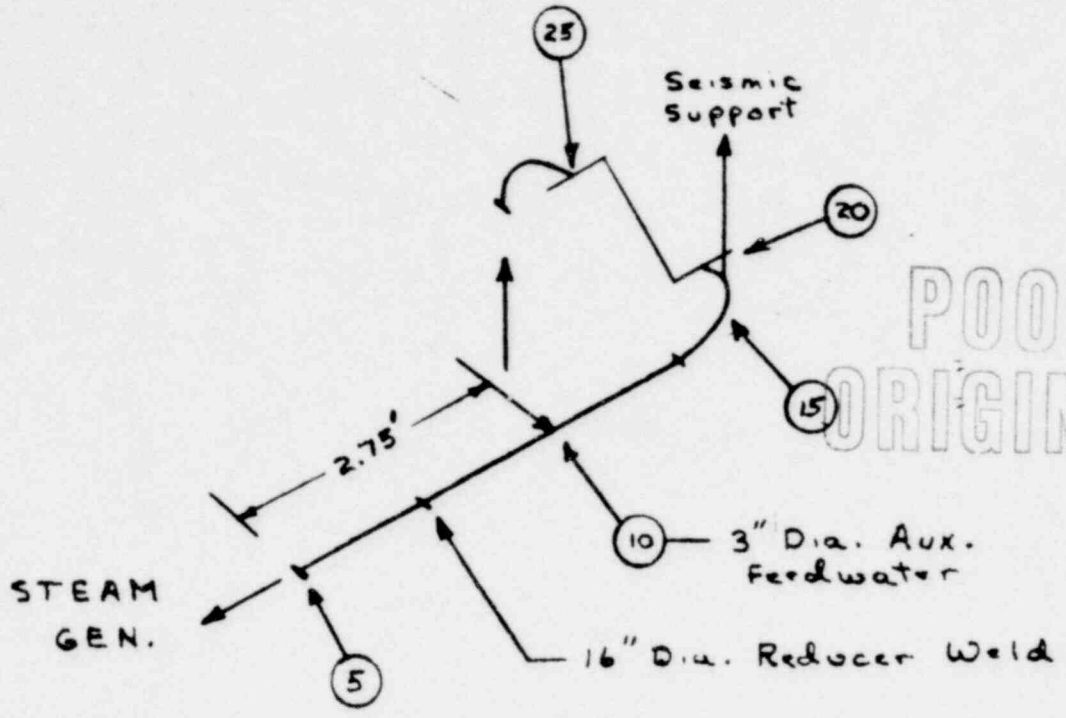

STRESS SUMMARY

Data Point	Thermal Stress, psi	Gravity Stress, psi	Longitudinal Pressure stress, psi	Total Seismic Stress, psi OBE	SSE	REMARKS
5	4736	104	3608	5059	6406	Nozzle
10	4163*	65*	3608	8138*	12603*	Aux. F.W. Connec.
15	6804	90	3608	5719	7740	Elbow
20	5934	183	3608	4159	4527	End Bend
25	5993	104	3608	4031	4350	Begin Bend

*Stress intensification factor not included.

FIGURE 2

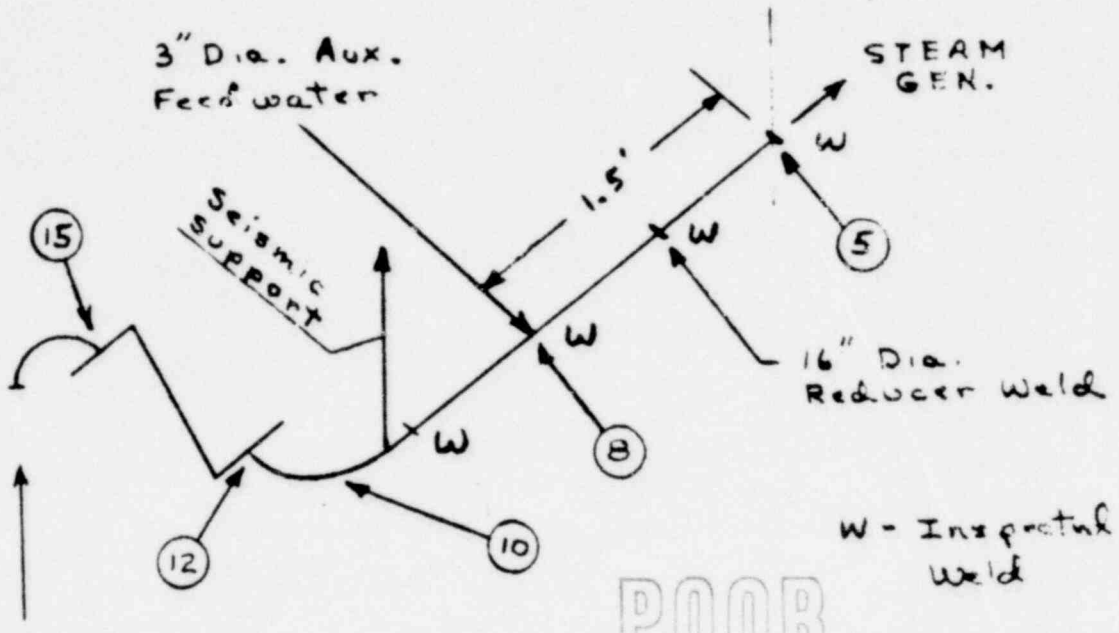

STRESS SUMMARY

Data Point	Thermal Stress, psi	Gravity Stress, psi	Longitudinal Pressure stress, psi	Total Seismic Stress, psi OBE	SSE	REMARKS
5	1730	3000	3608	9692	12776	Nozzle
3	3114*	3000	3608	7559*	8510*	Aux. F.W. Connec.
10	3114	3000	3608	11143	15678	Elbow
12	2129	3000	3608	7566	8524	End Bend
15	126	3000	3608	7379	8150	Begin Bend

*Stress intensification factor not included.

FIGURE 3

CALCULATION SHEET

SHEET - OF -

FILE No

SUBJECT POINT BEACH NUCLEAR PLANT MADE BY DATE

MAIN FEEDWATER - Unit 2, "B" CHKD. BY DATE

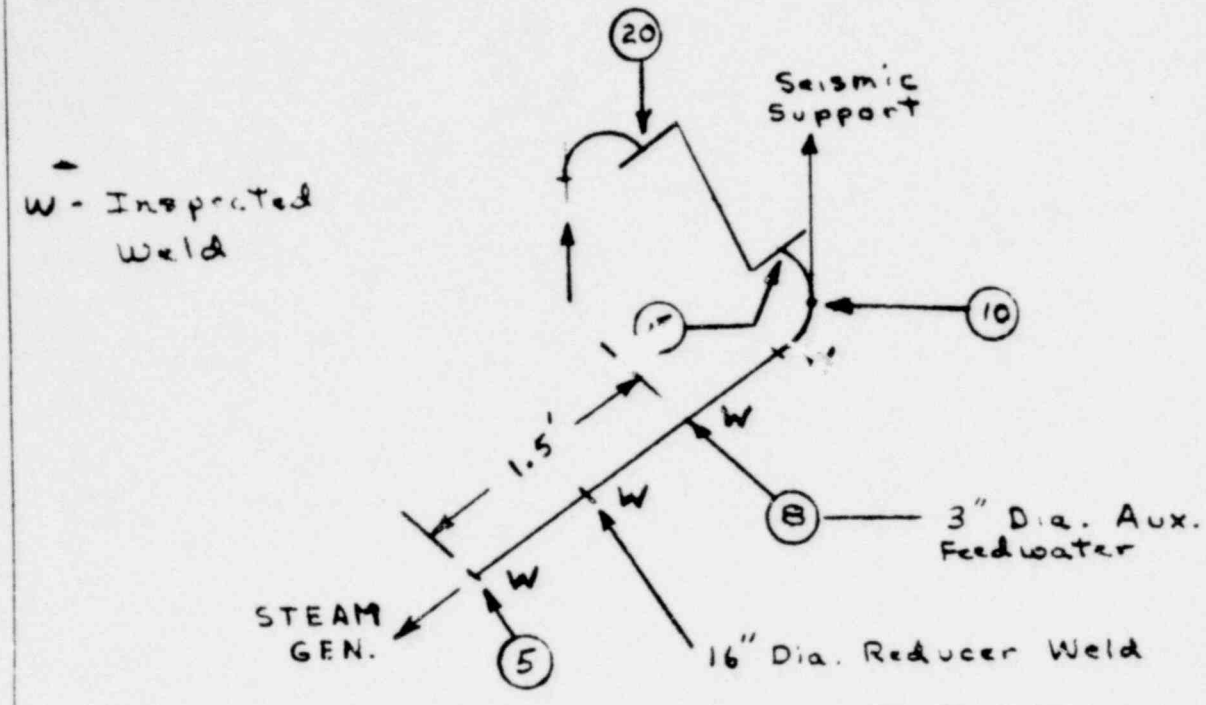

STRESS SUMMARY

Data Point	Thermal Stress, psi	Gravity Stress, psi	Longitudinal pressure stress, psi	Total Seismic Stress, psi OBE	SSE	REMARKS
5	4613	3000	3608	8066	9524	Nozzle
8	5127*	3000	3608	7893*	9358*	Aux. F.W. Connec.
10	11331	3000	3608	8636	10664	Elbow
15	971	3000	3608	6976	7344	End Bend
20	7433	3000	3608	7059	7510	Begin Bend

*Stress intensification factor not included.

FIGURE 4

TABLE 1

LIST OF SIGNIFICANT OPERATING EVENTS FOR FEEDWATER PIPING SYSTEM TRANSIENTS AUGUST 24, 1979

POINT BEACH NUCLEAR PLANT UNIT 1

DATE	EVENT
7/70	Hot functional test completed.
11/2/70	Initial criticality.
11/22/70	Turbine trip from 40% power.
11/29/70	Power escalation to 70% and unit trip.
12/4/70	Turbine and reactor trip from 425 MWe.
12/6/70	Manual unit trip from 70% power.
12/18/70	Unit trip from 80% power.
12/19/70	Unit trip from 35% power (loss of feedwater).
1/4/71	Auxiliary feedwater injection during plant startup.
1/8/71	Unit trip from 82% power.
1/9/71	Turbine trip from 70% power.
1/27/71	Unit trip from 90% power.
1/28/71	Turbine trip from 92% power.
1/29/71	Unit trip from 72% power.
2/3/71	Turbine trip from 90% power.
2/4/71	Unit trip from 90% power plus a turbine trip.
2/9/71	Unit trip from 80% power.
2/26/71	Load runback from 450 MWe to about 200 MWe.
7/2/71	Reactor and turbine trip.
8/29/71	Reactor and turbine trip.
9/7/71	Load runback from 425 MWe to 260 MWe.
9/18/71	Load runback from 480 MWe to 390 MWe.
12/3/71	Reactor and turbine trip.
1/3/72	Reactor and turbine trip.
1/19/72	100% load rejection test (reactor and turbine trip).
2/13/72	Load runback of 20%.
4/13/72	Load runback of 20%.
4/21/72	Reactor and turbine trip.
7/3/72	20% step increase in power.
9/11/72	Turbine and reactor trip from 99% power.
5/18/73	Unit trip from 72% power.
7/2/73	Reactor and turbine trip.
8/11/73	Reactor and turbine trip.
1/11/74	Reactor and turbine trip.
1/18/74	Reactor and turbine trip.
2/3/74	Reactor and turbine trip, preceded by a turbine runback.
8/2/74	Reactor and turbine trip from 430 MWe.
9/25/74	Reactor trip from 99% power.
10/4/74	Reactor and turbine trip.

TABLE 1 PBNP UNIT 1 - CONT'D
AUGUST 24, 1979

DATE	EVENT
2/27/75	Emergency shutdown with reactor and turbine trip.
11/16/75	Emergency shutdown with reactor and turbine trip.
1/10/76	Load runback of 20%.
1/14/76	Reactor trip.
11/30/76	Load runback from 90% to 70% power.
2/21/77	Reactor and turbine trip.
4/6/77	Reactor and turbine trip.
1/7/78	Reactor and turbine trip from 99% power.
2/9/78	Reactor and turbine trip from 99% power.
4/2/78	Reactor and turbine trip from 99% power.

TABLE 2

LIST OF SIGNIFICANT OPERATING EVENTS FOR FEEDWATER PIPING SYSTEM TRANSIENTS AUGUST 24, 1979

POINT BEACH NUCLEAR PLANT UNIT 2

DATE	EVENT
12/22/71	First unit heatup, normal.
5/30/72	Initial criticality, power restricted to 1%.
7/28/72	20% power authorized.
8/3/72	Unit reaches 20% power.
8/4/72	Turbine trip from 20% power.
8/18/72	Unit trip from 10% power.
8/30/72	Load swing test 20% to 14% to 20%.
8/31/72	Unit trip from 20% power.
12/7/72	Turbine trip from 20% power plus a turbine and reactor trip from 10% power.
1/14/73	Reactor and turbine trip from 20% power.
2/18/73	Reactor and turbine trip from 20% power.
3/8/73	Received 100% power license.
3/9/73	Reactor and turbine trip, from 50% power.
3/10/73	Reactor and turbine trip.
3/14/73	Reactor and turbine trips - 2; one from 390 MWe.
3/24/73	Reactor and turbine trip from 92% power.
3/26/73	Reactor and turbine trip.
3/30/73	Reactor and turbine trip from 70% power.
4/8/73	Reactor and turbine trip.
5/30/73	Reactor and turbine trip.
6/19/73	Reactor and turbine trip.
10/13/73	20% load runback.
12/15/73	Reactor and turbine trip from 100% power.
12/27/74	Reactor and turbine trip from 430 MWe.
2/11/75	Reactor and turbine trip.
2/24/75	Reactor trip from 10% power.
8/19/75	Reactor trip from about 10% power.
1/14/76	Manual unit trip.
2/21/76	Load runback of 20%.
4/8/76	Unit trip.
5/7/76	Load runback of 20%.
6/13/76	Load runback from 100% to 80% power.
9/3/76	Reactor trip.
1/12/77	Reactor and turbine trip.
6/28/77	Reactor and turbine trip.
7/7/77	Reactor and turbine trip.
1/10/78	Reactor and turbine trip from 60% power.
12/9/78	Reactor and turbine trip from 99% power.
4/11/79	Manual unit trip from 22% power.

Bechtel Power Corporation
Engineers—Constructors
Fifty Beale Street
San Francisco, California
Mail Address: P.O. Box 3965, San Francisco, CA 94119

Project File No. 10447-004
079-48

August 17, 1979

Mr. D. K. Porter
Superintendent - Nuclear Projects Office
Wisconsin Electric Power Company
231 West Michigan
Milwaukee, Wisconsin 53201

Attention: Mr. D. Dill

Subject: Bechtel Job No. 10447
Point Beach Nuclear Plant
Auxiliary Feedwater Line Temperature Distribution

Dear Mr. Dill:

On August 13, 1979, you requested that we provide a steady state temperature distribution in the 3 inch auxiliary feedwater line.

We prepared a calculation for this request with the following assumptions and results:

Main Feedwater Line (16 inch) temperature	420° F.
Auxiliary Feedwater (3 inch) line condition	Stagnant (no flow)

The calculation was based on a cooling fin model assuming that the outside heat transfer coefficient is constant over the length of the pipe. We also calculated a single thermal conductivity that represents the pipe, water and insulation.

The insulation of the 3 inch auxiliary feedwater piping consists of 1 inch fiber glass. This is based on the records we have. If thicker or different insulation is installed then these results are not conservative. The 3 inch pipe is also considered to be in the horizontal plane which is conservative.

For conservatism we assumed that the feedwater is mixed and at 420° for one foot into the 3 inch auxiliary feedwater line.

The maximum length to where the 3 inch pipe wall temperature reaches 150° F. under the above conditions is three (3) feet. This temperature is essentially ambient conditions in the containment near the piping. Attached are the temperature distribution curves for two auxiliary feedwater lines.

We trust this satisfies your request. If there are any questions, please call me.

Very truly yours,

J. R. Buell for
D. H. Clark
Project Engineer

CBH:ba
Enclosure

1044 247

Figure 5.

Detail of TEMP. PROFILE 3IN-226 FT. 2Hx1A

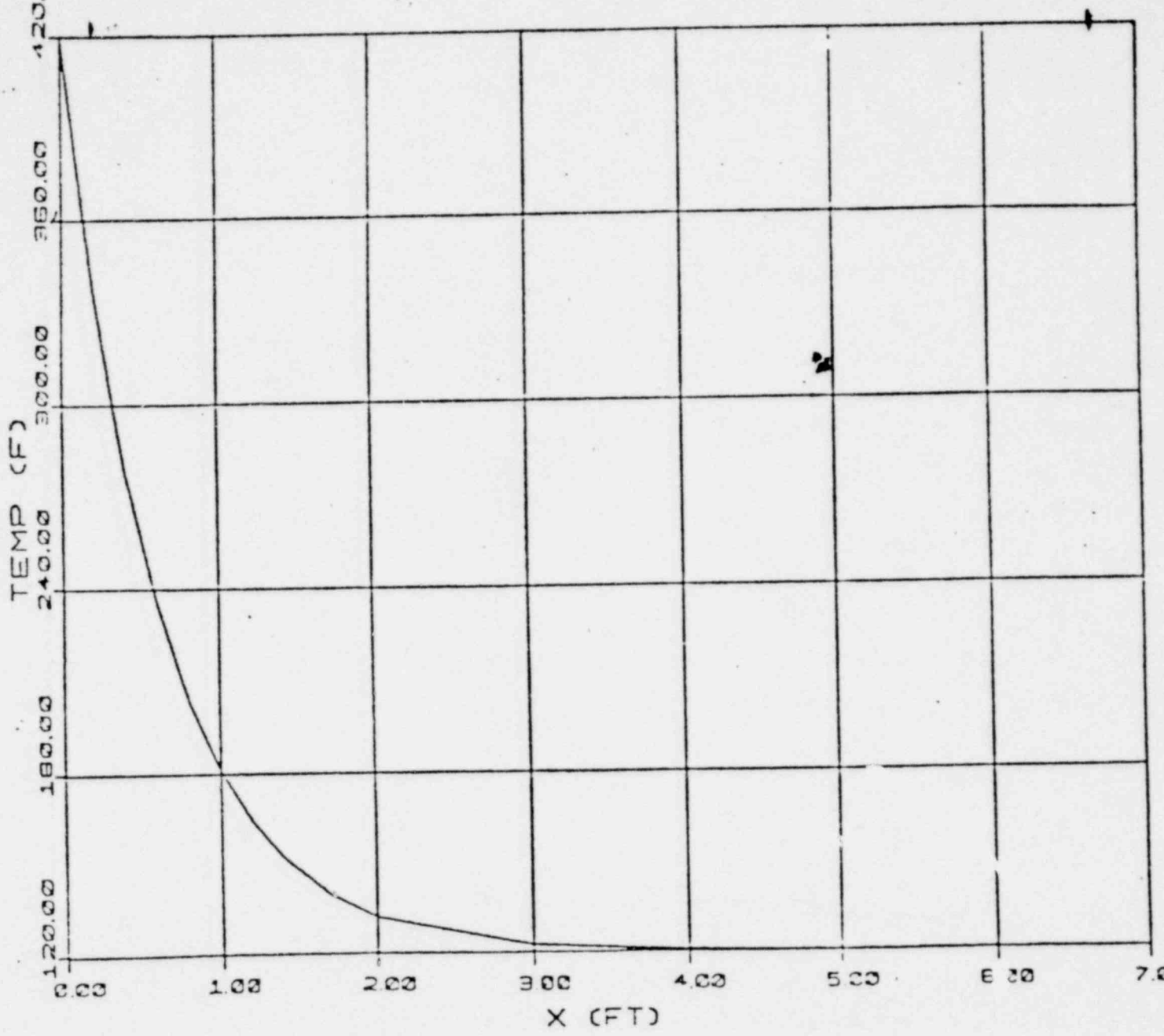

CAM:58-79
10447010-500Z(0)
MK 8-16-79

Figure 3. DETAIL OF 3 IN., 58 FT.

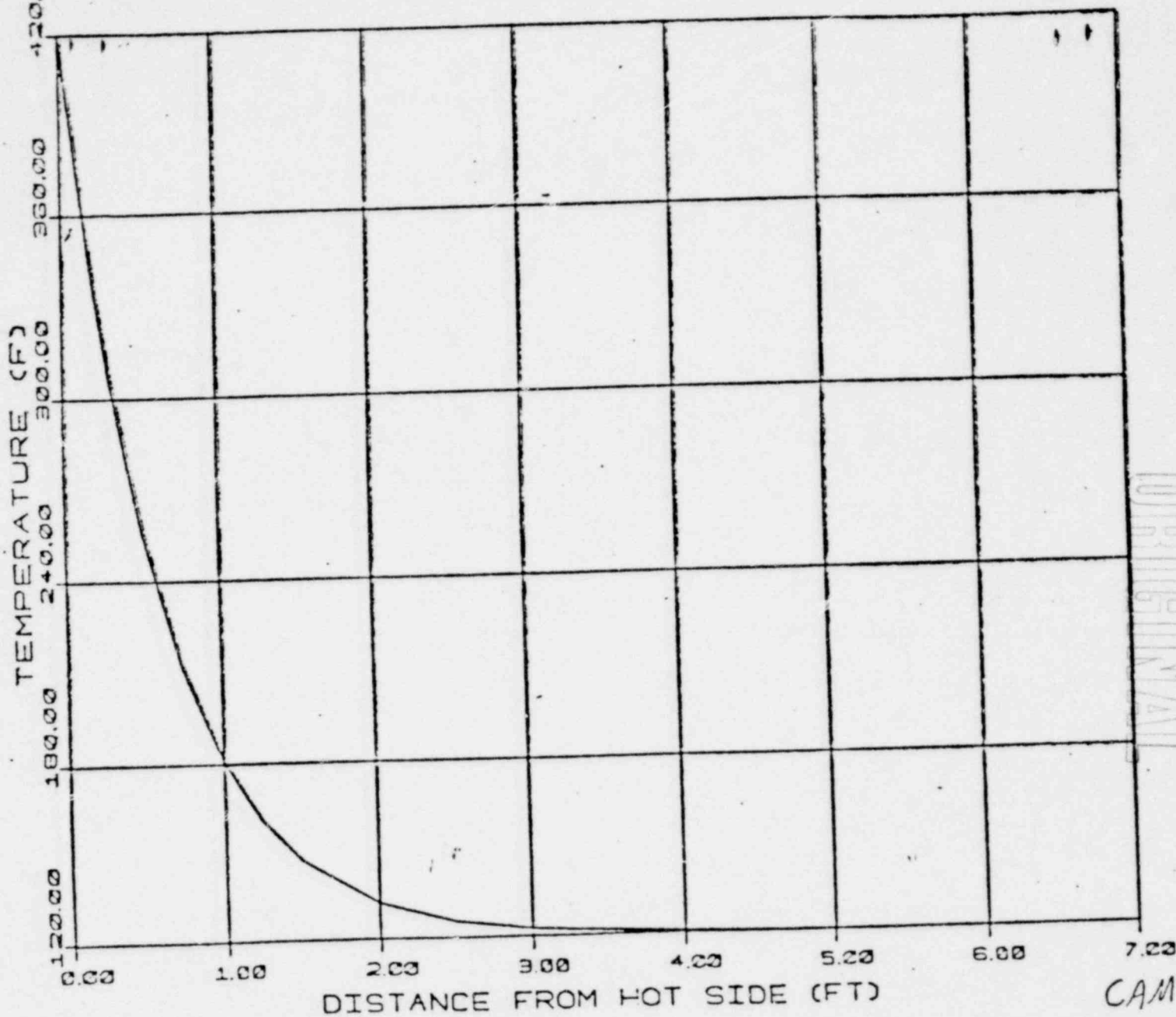

CAM: 58-79
10447010.5002(0)
MH 8-16-79

APPENDIX B

METALLURGICAL EVALUATION OF FEEDWATER PIPE CRACKING

METALLURGICAL EVALUATION OF FEEDWATER PIPE CRACKING

INTRODUCTION

On July 5, Southwest Research Institute (SwRI) was supplied one 18-in. X 16-in. reducer removed from the "A" steam generator of Point Beach Nuclear Plant, Unit 2. The reducer was removed by cutting through the 18-in. reducer-to-nozzle and the 16-in. pipe-to-reducer welds. Cutting was performed without the use of lubricants. The cut passed through the weld crown at the O.D. at both the 18-in. and 16-in. ends. At the I.D. of the 18-in. end, the cut passed through the root-pass weld bead or in the heat-affected zone (HAZ) of the reducer. At the I.D. of the 16-in. end, the cut passed through the weld bead or in the HAZ of the pipe.

On July 18, an additional sample was also submitted for analysis. This sample was removed from a feedwater pipe of the "B" steam generator of the same unit. The sample contained a crack and was removed as a consequence of radiographic and ultrasonic inspection of repair welds to the feedwater piping system.

Radiographs performed at Point Beach by Superior Industrial X-ray Corporation and interpreted by Mr. S. Wenk of SwRI showed a crack-like indication from station marker #10 to #16 (63° - 100°) near the 18-in. reducer to nozzle weld. Two transverse indications 1/4 in. long were also detected at stations #42 and #43 running from the weld crown into the reducer base metal. Three linear indications were also detected at the 16-in. pipe-to-reducer weld on the pipe side.

Before removing any material from the reducer, ultrasonic inspection was performed to more accurately position the defect causing the RT indications at the 18-in. end. This examination confirmed the existence of a flaw which was clearly present from stations #10 to #21 (62° - 130°) and #23 to #25 (144° - 157°). The flaw was positioned approximately 3/8 in. from the end of the reducer, that is, in the vicinity of the transition from the counter-bore to full reducer I.D. Only the section from stations #8 to #26 was examined using ultrasonics. After location of the flaw giving rise to the RT indications, a ring 1-1/2 in. to 2 in. wide was cut from the

18-in. end of the reducer. No lubricant was employed during this or any subsequent cutting operation. The ring was then cut in half, through stations #0 and #28, 0° and 180°. Each half was examined visually using a stereoscopic microscope at magnifications up to 50X. A similar ring was also removed from the 16-in. end of the reducer.

No crack could be unambiguously identified at the counter-bore transition. In the zone from station #10 to #20 the oxide was unusually rough and porous in appearance. Over most of the circumference the oxide at the counter-bore transition was not noticeably different from that in other regions. Randomly distributed pit-like areas were present, but were not grouped linearly as at stations #10-#20. Cracks could be positively identified at the root pass fusion line at stations #37 - #37.5, #42 - #45, and #45.5 - #49 (~230° and 260° - 319°), Figure 1. No evidence of cracks corresponding to the transverse RT indications could be seen at station #42. However, two stamped marks on the O.D., adjacent to the weld crown, could be responsible for these indications.

The oxide was electrolytically removed from selected segments to examine the underlying surface. On the 18-in. end copious cracking was observed at and near the counter-bore transition, that is, at the intersection of the flat counter-bore and bevelled counter-bore regions, Figure 2. Most cracks were situated at the root of machining grooves, at the root-pass fusion line or at the base of deep pits. No cracks in an axial orientation could be found in the base metal, although several small axial cracks were present on the weld bead, Fig (b). As will be seen below, no cracks were observed at the HAZ in r rgical sections. Macroscopic examination showed that grinding the weld bead had virtually removed the machining marks in this area, Figure 3. Some small cracks were present in the HAZ, Figure 3(b), at pits or small grooves. Thus, the general absence of cracks in the HAZ is attributed to the elimination of stress-raisers, rather than to metallurgical structure or residual stress effects.

Examination of the 16-in. end by magnetic particle inspection did not reveal any definite crack-like indications. Two weak indications were obtained at the fusion line of the root pass at stations #14 and #41 (100° and 295°). Before oxide removal no cracks could be seen. After partial removal of the oxide by cathodic polarization in Endox, a definite copper-colored line could be seen at the counter-bore transition, Figure 4. Similar copper-colored deposits could also be seen at pits in the weld bead and reducer section. Energy dispersive X-ray analysis positively identified the deposits as elemental copper, Figure 4(b). After thorough cleaning, small cracks could be seen at the weld fusion line and at the counter-bore transition. Cracking was much less profuse than at the 18-in. end. Cracks were rarely present in machine grooves other than that which constituted the transition.

A second distinct groove was also present at the 16-in. end about 2-7/32 in. from the weld fusion line. This groove appears to have been created by a final machining pass restricted to this end of the reducer. A few minute cracks could be found in this area by careful visual inspection at 50X magnification after complete cleaning. No other cracks could be found in other parts of this section.

Several areas of the reducer I.D. remote to the counter-bore were carefully inspected for either axial or circumferential cracks. Particular attention was given to areas at the 18-in. end where the surface contained gouges in the axial direction. No evidence of axial cracks could be found. One extremely small circumferential crack, less than 0.001 in. long, was found at the base of a large pit at the 18-in. end. No other cracks were observed.

METALLOGRAPHIC ANALYSIS

The structure of the reducer and welds was normal for mild steel piping, Figure 5. No metallurgical abnormalities such as islands of martensite, heavy banding or gross inclusions were observed. Sections at stations #11, #14, and #41 (80°, 100° and 295°) of the 16-in. end revealed a lack of fusion defect between the first and second passes, Figure 6.

In some sections this defect also contained oxide inclusions. This indicates that insufficient shielding of the first pass and insufficient heat input during the second pass were employed during deposit of the original reducer-to-pipe weld. Despite the size of these defects, there was no evidence that flaw growth had occurred.

Cracks were found in all longitudinal sections taken from the counter-bore region of the 18-in. end of the reducer. The depth of the largest crack and the number of cracks in each section are given in Table I. In all cases multiple cracking was observed, Figures 7 and 8. Cracks were observed over the entire counter-bore region from the weld fusion line to the counter-bore transition. Cracks were also present for some distance up the bevel of the counter-bore, Figure 8(a), but no cracks were found at the unmachined reducer I.D., Figure 9. Cracks were found at the weld fusion line, Figure 10, in sections from stations #0, #10, #19, and #43. These were the only sections in which the root-pass fusion line was present. In general, these cracks were oxide filled, similar to those in the counter-bore. Only those cracks which could be seen visually near #43 were wide at the mouth.

To characterize the small axial cracks on the root-pass weld bead, transverse serial sectioning was performed. Typical defects and the deepest defect found are shown in Figures 11(a) and 11(b), respectively. No cracks similar to those observed in the fusion line or counter-bore could be seen. It is worth noting that this section was electrolytically cleaned to remove the oxide prior to mounting. The same technique was also employed on sections from the 16-in. end of the reducer. As can be seen in Figure 12, this procedure did not remove the oxide from within tight cracks. Fractographic examination of specimens, which had been cleaved open and electrolytically cleaned, showed that no dissolution of the base metal had occurred. It can, therefore, be assumed that the defects observed in the weld bead were different from those in the base metal. It is most likely that the crack-like defects were formed during the welding and were subsequently corroded.

TABLE I

NUMBER AND DEPTH OF CRACKS AT 18-IN. REDUCER END

Section	Maximum Depth (in.)	Number of Cracks Deeper than 0.002 in.
# 0	0.040	3
#10	0.018	8
#15	0.043	13
#19	0.026	7
#22	0.014	4
#25	0.004	1
#28	0.008	3
#34	0.007	2
#43	0.042	7

Two sections were taken from stations #14 and #41 of the 16-in. end where a careful magnetic particle test had indicated cracks at the weld fusion line on the reducer side of the weld. Cracks could be seen at both sides of the fusion line. These cracks were tight, oxide filled and branched, Figure 10(b). No cracks or oxide spikes were present in the counter-bore region. Sections were therefore taken at areas where visual examination showed cracks. Included for examination were the weld bead, transition zone and the step 2-7/32 in. from the weld. Micrographs showing typical cracks observed are shown in Figure 12.

Detailed examination of crack tips showed that they are invariably blunt and oxide filled, Figures 7 through 13. On many cracks, oxide spikes propagated perpendicular to the crack for a considerable distance into the base metal, Figures 8 and 13. This behavior was not microstructurally dependent, and must thus be attributed to changes in plant operating conditions which caused crack arrest for a prolonged period of time. In general, the oxide within the cracks was dense for a considerable distance from the crack-tip, Figure 13. In some cases, however, open fissures did extend in the oxide from the surface to the crack-tip, Figures 8 and 10. The Pillings-Bodsworth* ratio for the oxidation of iron is always greater than 1, so that the oxide would tend to fill cracks even under the influence of a moderate mean stress. The cracks in which the oxide was fissured were deeper than others in the section. The possibility that stresses applied during reducer removal may have opened these cracks cannot be ignored. It is thus difficult to draw any conclusions based on this observation.

A transverse section through the sample received on July 18 is shown in Figure 14. The defect lies at a large angle to the pipe surface, as predicted from the UT examination performed by SwRI. The fissure was oxide filled and surrounded by a decarburized layer. Note that the pipe O.D. was not decarburized. No distinct interface existed between the decarburized and normal zone, Figure 14(b). Upon opening, the oxide was found to be powdery and nonadherent. These characteristics are typical of a rolled-in or forged-in lap. It is, therefore, concluded that this defect was present prior to welding and resulted from the pipe fabrication process.

* The ratio of the oxide to metal volume.

FRACTOGRAPHIC EXAMINATION

Specimens were taken adjacent to stations #15 and #43 of the 18-in. end for fractographic examination. Specimens were notched behind the counter-bore transition and broken open, Figure 15. Beach markings could be seen in several locations, Figure 15(c), indicative of periodic crack arrest. All cracks were heavily oxidized. Even at the transition to laboratory cleavage fracture no detail could be seen, Figure 16(b). In some areas, the fracture surface appeared to be intergranular, Figure 16(a), but electrolytic cleaning removed all such features. The cleaning procedure did not alter the appearance of the cleavage fracture. The intergranular facets are therefore attributed to the oxide morphology. After cleaning, the surface of in-service cracks was pitted in appearance, Figure 16(c), but did not show signs of fatigue striations.

Energy dispersive X-ray analysis was performed on each of the fracture surfaces before electrolytic cleaning. For comparison, spectra were also collected on the region of laboratory overload. Iron was always the primary peak observed on the in-service fracture, Figure 17. Small peaks indicating traces of phosphorus, sulphur, manganese and copper were also usually observed. An additional peak corresponding to titanium, but slightly shifted in energy, was also observed. Comparison with the spectrum from the cleavage fracture, Figure 17(c), indicated that the iron, manganese and titanium peaks originated from the base metal. The remaining elements, phosphorus, sulphur and copper must be attributed to service exposure. These peaks are not unexpected. Coordinated phosphate water treatment was used at Point Beach for some time, accounting for the presence of phosphorus. Copper from corrosion of condenser and heat exchanger tubes is also commonly found deposited on steel components, since iron displaces copper in solution according to the reaction:

$$Cu^{2+} + Fe \longrightarrow Fe^{2+} + Cu$$

Copper in solution therefore acts as a cathodic species. Sulphate is known to be a common species in turbine deposits[1] and, therefore, the presence of sulphur is not surprising. No evidence of halides was detected on any of the

specimens examined. On one sample a small nickel peak was also observed. Again, this is not surprising as nickel-base alloys are extensively used in steam generators.

In some samples phosphorus was observed near the crack mouth, but not at the crack tip. However, in one sample (at station #14 of the 18-in. end) very little phosphorus was observed.

One section from stations #11 to #11-3/4 of the 16-in. end was also broken open. This area was selected during visual examiantion as that containing the most obvious cracks. Several small cracks could be seen, but only four cracks, totaling less than 1/4 in. in length, exceeded 0.003 in. The deepest crack was 0.013 in. deep.

A large segment of the 18-in. reducer was subjected to crack sizing using the Satellite Pulse Technique developed at SwRI. The segment from station #11.5 to #15 was examined in detail and the crack depths plotted. Subsequently the segment from #14 - #15 was broken open and the crack depths plotted. The comparison of these data is given in Figure 8. From this data, it is apparent that the crack depth is less than 0.050 in. along the segment giving rise to the RT indications. It, therefore, seems unlikely that cracks significantly deeper than 0.050 in. exist elsewhere.

MECHANICAL TESTS

Charpy impact tests were performed to determine the fracture appearance transition temperature. Fourteen specimens were cut to simulate overload from the service cracking. The long axis of these specimens was longitudinal; the notch was cut parallel to the I.D. surface. In addition, four specimens were cut in the same orientation but with the notch perpendicular to the I.D. surface. Two specimens were cut with the long axis tangential and the notch parallel to the reducer I.D. The results of these tests are tabulated in Table II. Specimens notched parallel to the reducer I.D. often gave unreproducible results because of delamination in a plane parallel to the I.D. surface. No major delamination was observed in specimens notched perpendicular to the I.D. (samples 4-1 through 4-4) or in the two tangential specimens (2-1 and 2-2).

TABLE II

RESULTS OF CHARPY IMPACT TESTS ON REDUCER MATERIAL

Temperature, °F	Specimen+	Energy, ft-lbs.	Fracture Appearance*
440	V-3	191	D-L
440	V-4	167	D-L
220	V-1	155	D-L
220	V-2	150	D-L
75	V-5	166.5	D-L
75	V-6	133.5	D
50	V-13	132	D-L
50	V-14	107	10% B
32	V-7	125.5	D
32	V-8	47.5	70% B
0	V-9	30	95% B
0	V-10	155	D-L
-20	V-11	29.5	95% B
-20	V-12	32.5	95% B
100	4-2	96	20% B
75	4-1	76	30% B
75	4-4	84	30% B
50	4-3	56.5	80% B
100	2-2	72.0	D
75	2-1	44.5	80% B

+ All V-specimens cut with specimen axis longitudinal and notched parallel to I.D. All 4-specimens cut as above but notched perpendicular to I.D. All 2-specimens cut with specimen axis tangential and notched parallel to I.D.

* D: ductile
D-L: ductile with major delamination
B: brittle

SUMMARY OF FINDINGS

The crack-like RT indication at the 18-in. reducer end was found to correspond to shallow, oxide filled cracks. No cracks deeper than 0.047 in. were seen.

Cracks were deeper and more numerous at the 18-in. end than at the 16-in. end.

The deepest cracks observed in any section at the 18-in. end were always at the counter-bore transition zone. At the 16-in. end, cracks initiated at the weld fusion line were deeper than elsewhere.

Cracks were wide, oxide filled and frequently branched. No microstructural dependence was observed.

Cracks were invariably circumferentially oriented. No cracks were detected on the full reducer I.D.

Beach markings were observed on the oxide-covered fracture surfaces, but no fatigue striations could be found.

No anomalous species were observed in the crack deposit.

A lack of fusion defect in the 16-in. reducer-to-pipe weld was the only microstructural abnormality seen.

The reducer has a FATT below 100°F. Above that temperature the energy-to-fracture a standard charpy specimen exceeds 100 ft-lbs.

DISCUSSION

Little work has been performed on the stress-corrosion cracking and corrosion fatigue of mild steel piping alloys in pure water. Weinstein has stress-corrosion cracked SA 106B and SA 333 Gr. 6 in 8 ppm O_2 water at 550°F at stresses above the yield stress.[2] However, slow strain rate tests indicated that susceptibility to cracking was sensitive to oxygen content, decreasing significantly as the O_2 level was reduced to 200 ppb. It is, therefore, probable that at the low oxygen levels present in PWR steam generator feedwater SCC would be extremely slow and require higher stresses than at 8 ppm O_2.

Several studies of the corrosion fatigue of pressure vessel steels and carbon steel piping alloys have been performed in BWR environments. These, in general, conclude that carbon steel behaves similarly to the quenched and

tempered grades (2-4). A significant R-ratio and frequency effect is observed. The threshold ΔK decreases with increasing R-ratio and a detrimental influence of very low frequencies is observed. The ASME guidelines for predicting crack growth rate have been found to be conservative (2-4). In one of these studies[3] significant crack branching was observed. In addition, it was reported that a thick oxide layer extended to the crack-tip.

Tests in PWR primary coolant environments have generally observed similar corrosion fatigue behavior (5-8): low frequencies and high R-ratios are detrimental. Again, some workers report that a significant amount of crack branching and oxidation occur (5,6). Similar behavior has also been observed in X-65 pipeline steel in water[9].

In view of the above, the cracking observed here is consistent with a corrosion fatigue crack growth mechanism. The branching observed does not necessarily indicate that stress-corrosion cracking is involved. The beach markings observed should not be interpreted as direct evidence of a corrosion-fatigue cracking mechanism, since such markings do not result from crack blunting on large stress excursions, but rather from crack-tip dissolution and changes in oxide morphology. Such marking could therefore be produced during stress-corrosion cracking provided that operating conditions periodically altered and changed the crack tip chemistry or stress state. There is thus no direct evidence that stress-corrosion cracking has not occurred, or that fatigue loading is involved in the fracture process. Based on the work of Weinstein[2] the possibility of stress-corrosion cracking in mild steel piping cannot be ignored. However, because of the low stress levels believed to exist in the feedwater piping system and the low oxygen levels, stress corrosion cracking is thought unlikely. Fatigue loadings have been theoretically predicted in the areas which have cracked, and thus corrosion fatigue is the prime choice for a cracking mechanism.

Several observations are believed to indicate that the cracks seen have been present for a considerable length of time. All crack tips were blunt and heavily oxidized. In addition, no fractographic detail, such as

fatigue striations, could be seen. The environmental conditions seen in service are not severely oxidizing, so it is probable that the cracks were slow moving to allow such extensive oxidation. To verify this supposition, comparison should be made with cracks observed in the plants which have experienced rapid crack growth with observable striations. Certainly it would seem that some of the cracks were present at the time when coordinated phosphate treatment was used, since definite phosphorus peaks could be identified in the X-ray spectra.

There is no indication that inappropriate water chemistry control was the cause of cracking. All the species detected are known to exist in PWR feedwater and do not represent a departure from normal practice. The heavy deposits of elemental copper selectively located at pits and crack mouths may be regarded as normal, since these are sites at which iron is exposed without a protective oxide. The degree of copper build-up is an indication that the reduction of copper ions has made a significant contribution to the iron oxidation process. Thus, the presence of copper ions in feedwater must be viewed as contributing to the failure. There is no evidence, however, that cracking would not occur in the absence of copper ions.

The absence of axial cracks must be viewed as significant, since it has been hypothesized that the cause of cracking is thermal stresses generated when colder feedwater enters the hot piping system. Such thermal stresses would be biaxial and thus, in the absence of a biasing stress, result in randomly oriented cracks. The presence of a biasing stress, axial in orientation, is also predicated by the absence of cracks at the full reducer I.D.

The stress level would be lower in this region than at the counterbore because of the thicker section. These results also imply that the cyclic stress amplitude is relatively small, below the threshold value for R = 0. All cracks were associated with stress raisers, so that the elimination of such geometries and reduction in the axial biasing stress may eliminate the problem in the future.

The results of the charpy tests indicate that reducer material has a fracture appearance transition temperature no greater than 100°F. Specimens taken to simulate overload of the in-service crack gave a wide scatter because of delamination in the plane parallel to the reducer I.D. Specimens 2-1 and 2-2 did not delaminate so that these tests should give a fair indication of the FATT for transverse specimens notched perpendicular to the reducer I.D. This is slightly higher than that for the longitudinal specimens, as is normally observed. These results indicate that the reducer material has high toughness at temperatures above 100°F. Thus, there is little likelihood of catastrophic fracture in this temperature range. At lower temperatures, however, there exists the possibility of propagating a brittle fracture.

CONCLUSIONS

The most probable cause of cracking is corrosion fatigue. Cracks are believed to have been present during the period when coordinated phosphate water treatment was used.

The association of all cracks with stress-raisers suggests that the fine polishing used in the repair procedure should significantly improve piping and reducer longevity.

The toughness of the reducer material at temperatures above 100°F and the ductility of carbon steel renders a catastrophic failure improbable.

REFERENCES

1. O. Jonas, "Turbine Steam Purity," Southeastern Electric Exchange, Washington, D.C., April 1978, Document STD E-1528.

2. D. Weinstein, "BWR Environmental Cracking Margins for Carbon Steel Piping," EPRI Joint Projects Review Meeting on BWR Pipe Cracking, October 19 and 20, 1978, Palo Alto, CA.

3. D. A. Hale, J. L. Yuen and T. L. Gerber, "Fatigue Growth in Piping and RPV Steels in Simulated BWR Water Environment," U.S. Nuclear Regulatory Commission, March 1979, NUREG/CR-0390.

4. M. Suzuki, et al., "The Environment Enhanced Crack Growth Effects in Structural Steels for Water Cooled Nuclear Reactors," The Influence of Environment on Fatigue, 161, Institute of Mech. Engr., London, 1977.

5. W. H. Bamford, "The Effect of Pressurized Water Reactor Environment on Fatigue Crack Propagation of Pressure Vessel Steels," ibid, page 51.

6. W. H. Bamford, D. M. Moon and K. V. Scott, "Effect of High-Temperature Primary Reactor Water on the Subcritical Crack Growth of Reactor Vessel Steels," HSST Quarterly Progress Report, Sept. 1977, ORNL/NUREG/TM-120.

7. T. Kondo, et al., "Fatigue Crack Propagation Behavior of ASTM A533B and A302B in High Temperature Aqueous Environments," HSST 6th Annual Information Meeting, Paper No. 6, April 1972.

8. T. R. Mager, J. D. Landes, V. McLoughlin and D. M. Moon, "The Effects of Low Frequencies on the Fatigue Crack Growth Characteristics of A533B Cl. 1 Plate in an Environment of High Temperature Primary Grade Nuclear Reactor Water," HSST Report No. 35, Dec. 1973.

9. O. Vosikovsky, "Fatigue Crack Growth in an X-65 Line Pipe Steel at Low Cyclic Frequencies in Aqueous Environments," ASME J. Engr. Materials and Technology, 97, Series H, No. 4, 1975.

2-37774 4X

(a)

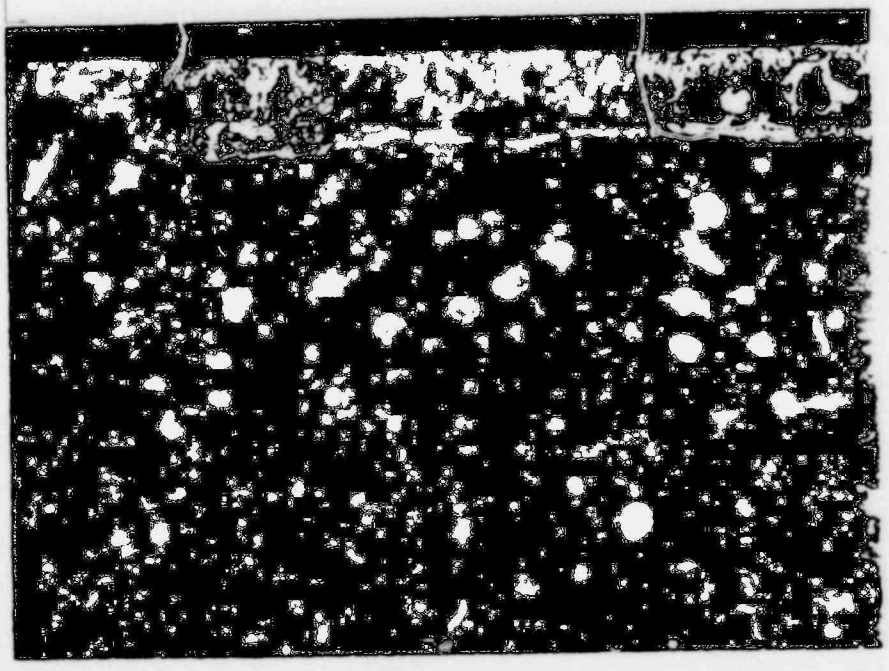

2-3[illegible] 4X

(b)

FIGURE 1. INTERNAL SURFACE OF REDUCER AT 18" COUNTER-BORE REGION. Note the fusion-line crack in 1(b), 1(a), #19-20 segment, 1(b), #44-45 segment.

2-37823 19X

(a)

2-37930 30X

(b)

FIGURE 2. INTERNAL SURFACE OF 18" END OF REDUCER AFTER ELECTROLYTIC CLEANING. Note that cracking occurs at the root of machine marks near the counter-bore transition, (a), #15. Small axial cracks were occasionally present on the weld bead, (b), #43, in addition to fusion-line cracking.

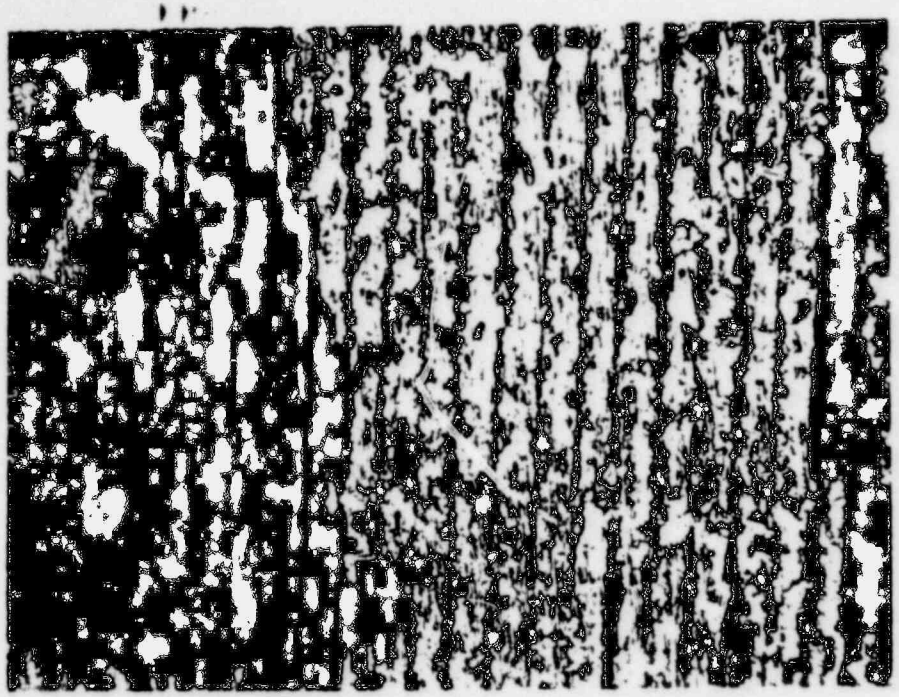

2-37827 10X

(a)

2-37825 51X

(b)

FIGURE 3. INTERNAL SURFACE OF REDUCER AT 18" COUNTER-BORE, THE WELD IS TO THE LEFT. Note that little cracking has occurred in the HAZ where grinding has removed the machining marks, (b).

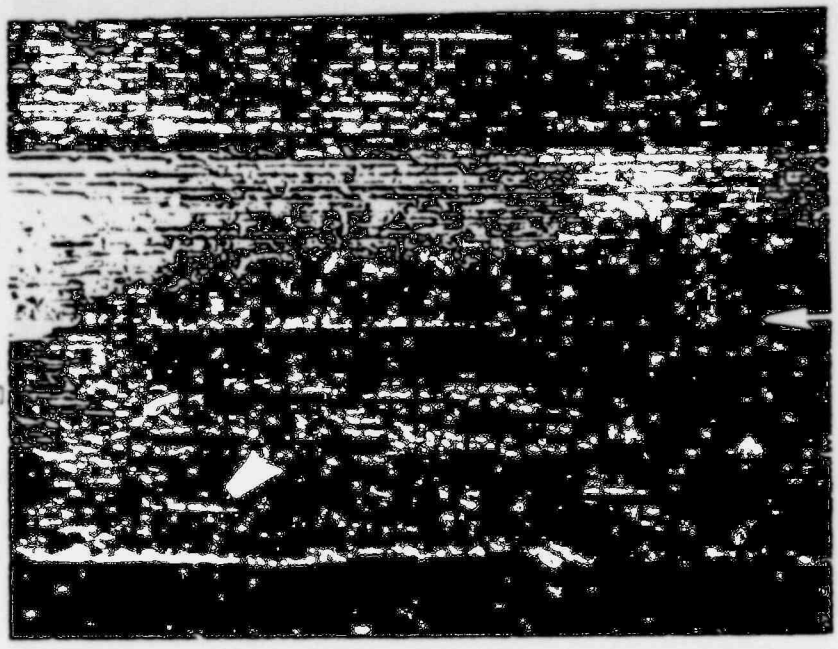

2-37977 3.5X

(a)

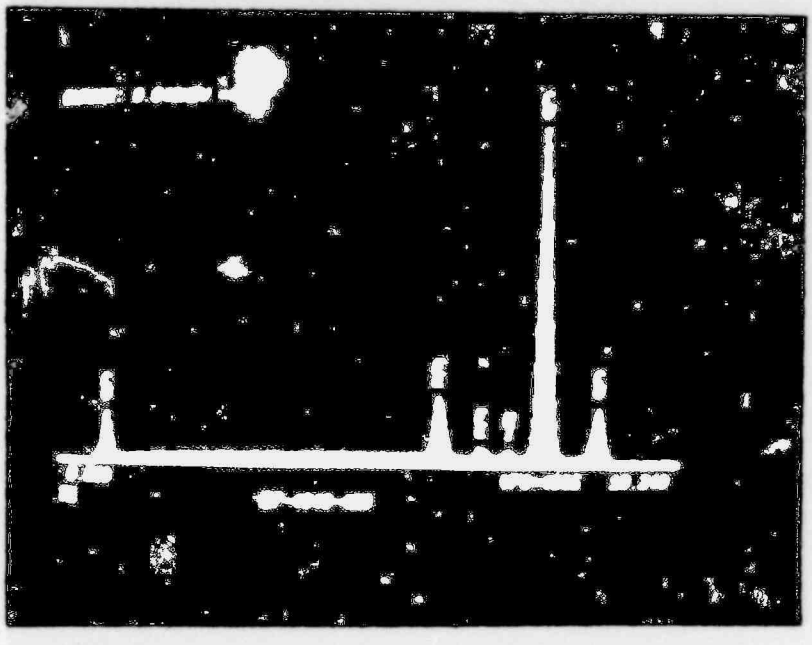

2-2136-S

(b)

FIGURE 4. COUNTER-BORE TRANSITION (ARROWED) OF 16-IN. REDUCER END AT WHICH A COPPER DEPOSIT (b) WAS OBSERVED AFTER SOME CLEANING.

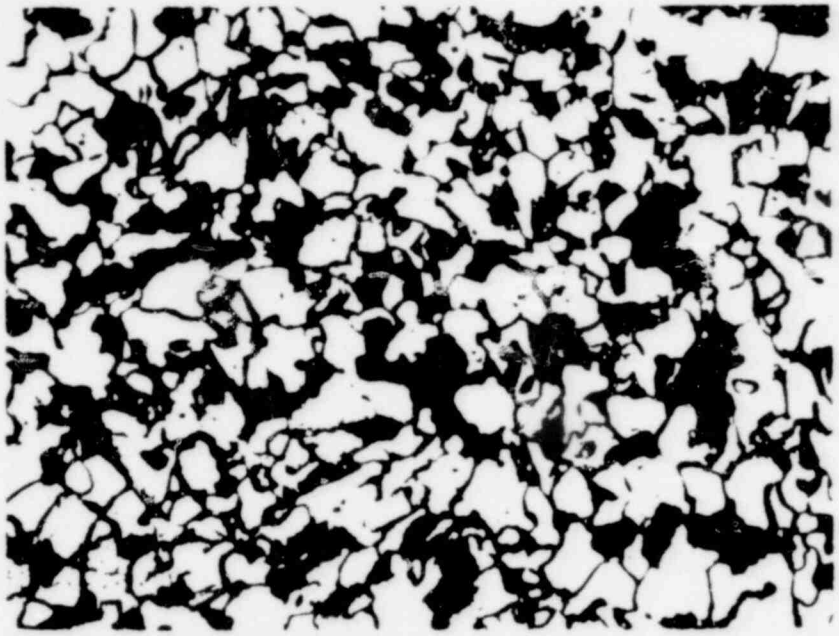

2-37658 500X

(a)

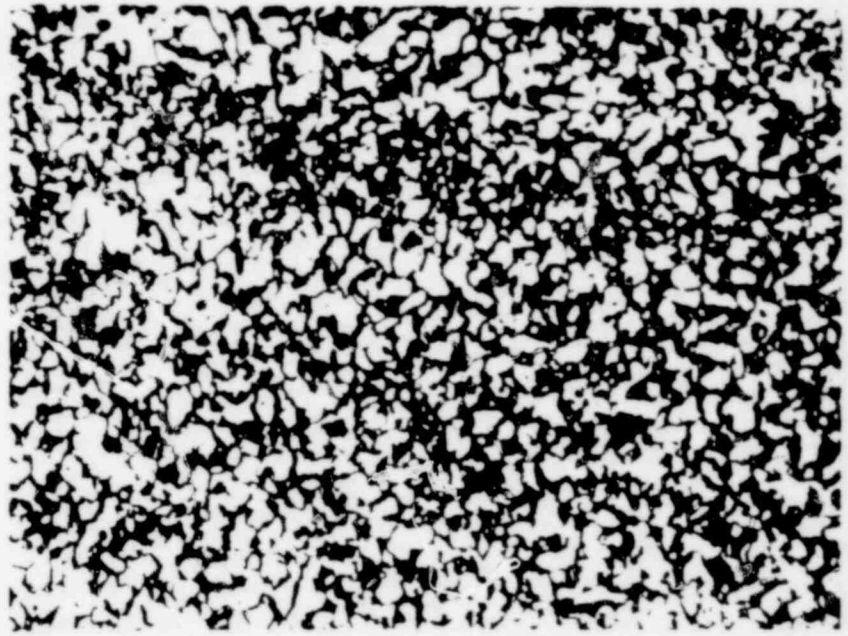

2-37660 500X

(b)

2-37661 100X

(c)

FIGURE 5. TYPICAL MICROSTRUCTURES OF REDUCER AND WELD. Base metal, (a), and heat-affected zone, (b), of reducer; Widmanstatten ferrite in weld bead, (c).

2-37936 4X

(a)

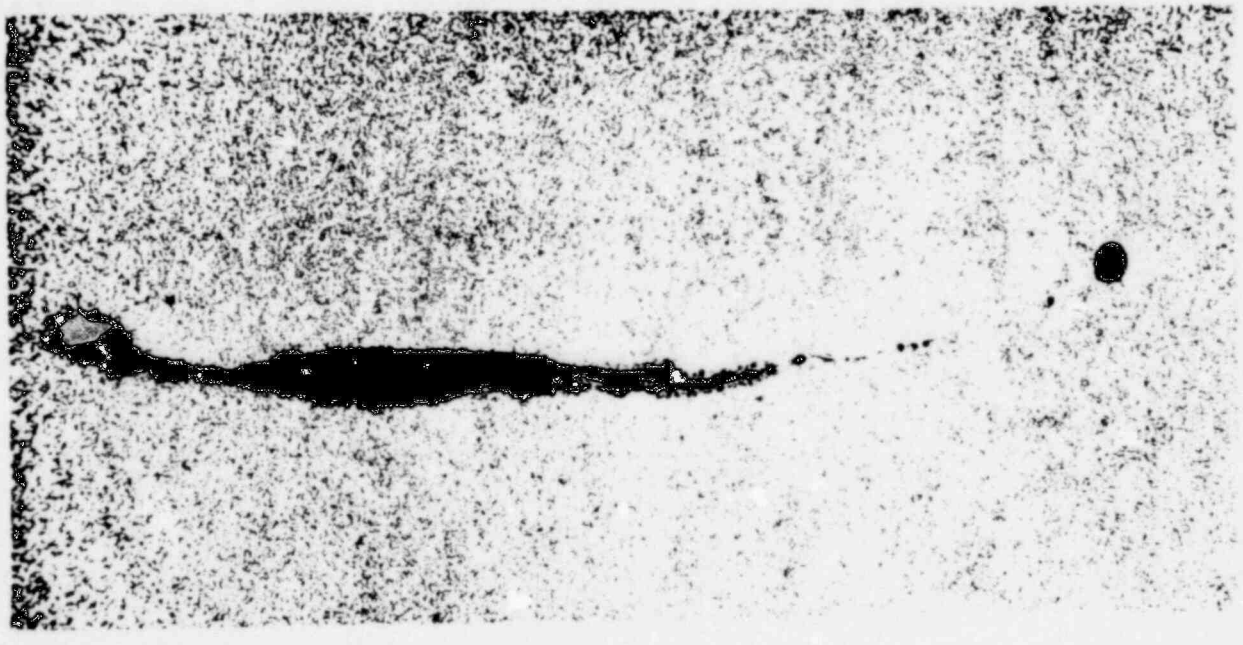

2-38114-115 50X

(b)

FIGURE 6. WELD DEFECTS IN THE 17-IN. REDUCER TO PIPE WELD. The arrows in (a) indicate the extent of the lack of fusion defect. In some sections oxide or slag inclusions could be seen, (b).

2-37791 300X

(a)

2-37789 50X

(b)

2-37617 50X

(c)

FIGURE 7. LONGITUDINAL SECTION OF 18" REDUCER AT, (a), AND, (b), STATION #19, (c), STATION #28.

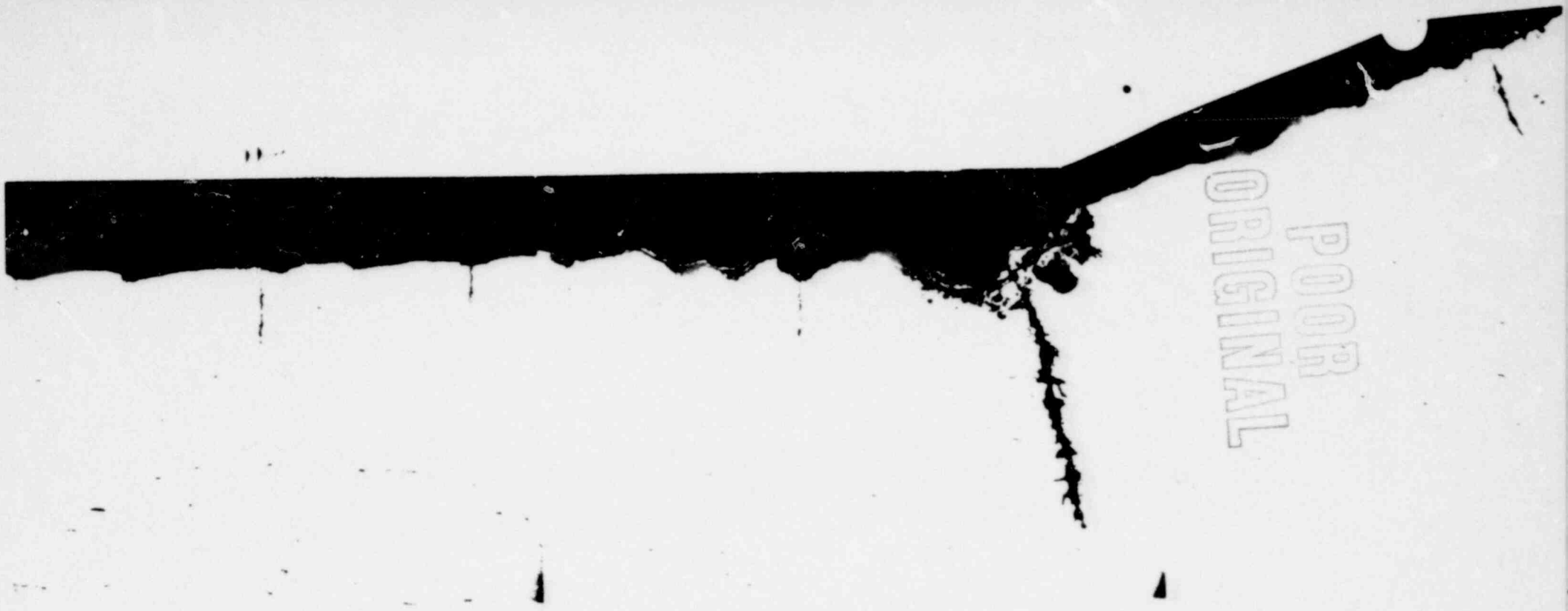

2-37622-24

50X

(a)

2-37627-28

50X

(b)

FIGURE 8. LONGITUDINAL SECTIONS AT STATIONS #15, (a), AND #43, (b), IN THE COUNTER-BORE TRANSITION ZONE. Note multiple cracks.

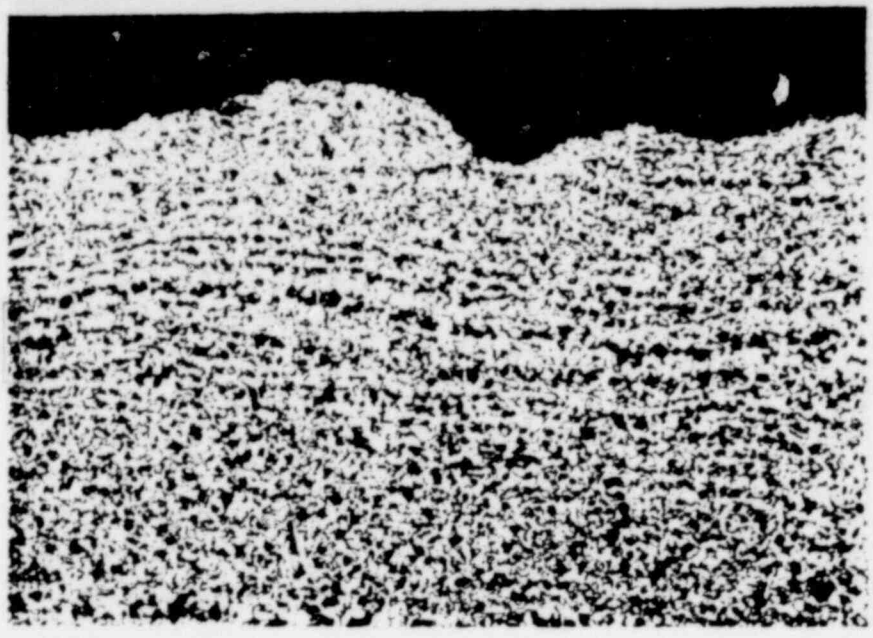

2-37822 100X

(a)

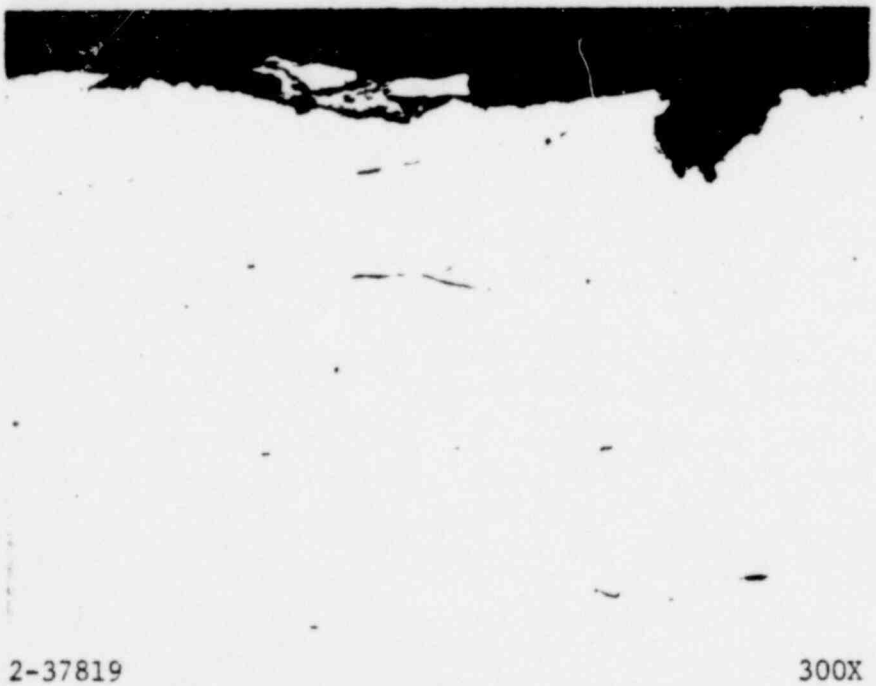

2-37819 300X

(b)

FIGURE 9. TRANSVERSE SECTION OF REDUCER I.D. AT STATION #17. Typical structure and surface finish, (a), and most severe attack observed, (b).

2-37626 50X

(a)

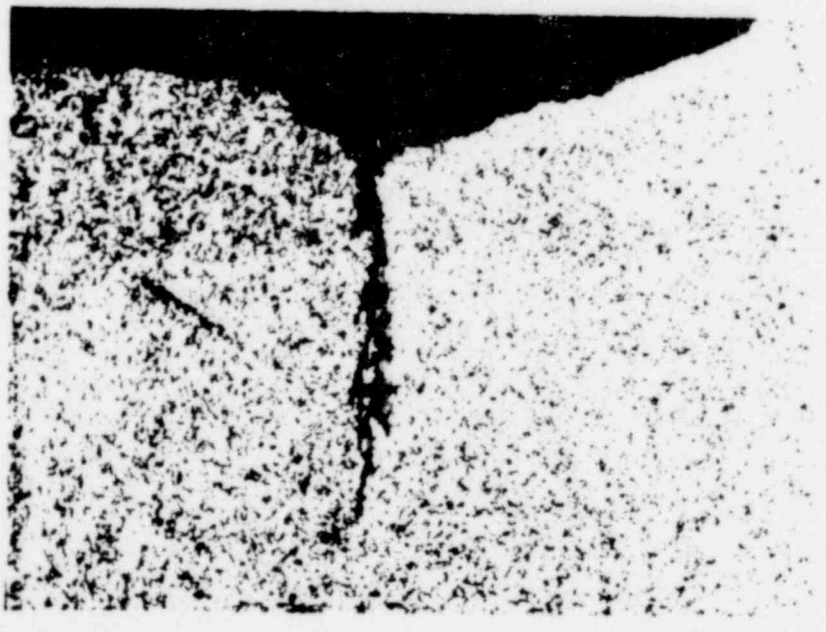

2-37934 100X

(b)

FIGURE 10. LONGITUDINAL SECTIONS AT THE REDUCER-NOZZLE, (a), AND REDUCER TO PIPE WELDS. The weld bead is on the left in (a) and the right in (b). Sections were taken at stations #43 and #14, respectively. Section (b), etched in nital.

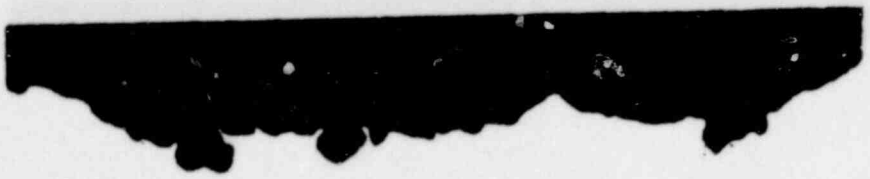

2-37937 150X

(a)

2-37941 250X

(b)

FIGURE 11. TRANSVERSE SECTIONS THROUGH THE WELD BEAD AT STATION #43, SHOWN IN FIGURE 2(b). No deep cracks, similar to those observed in the base metal, could be found.

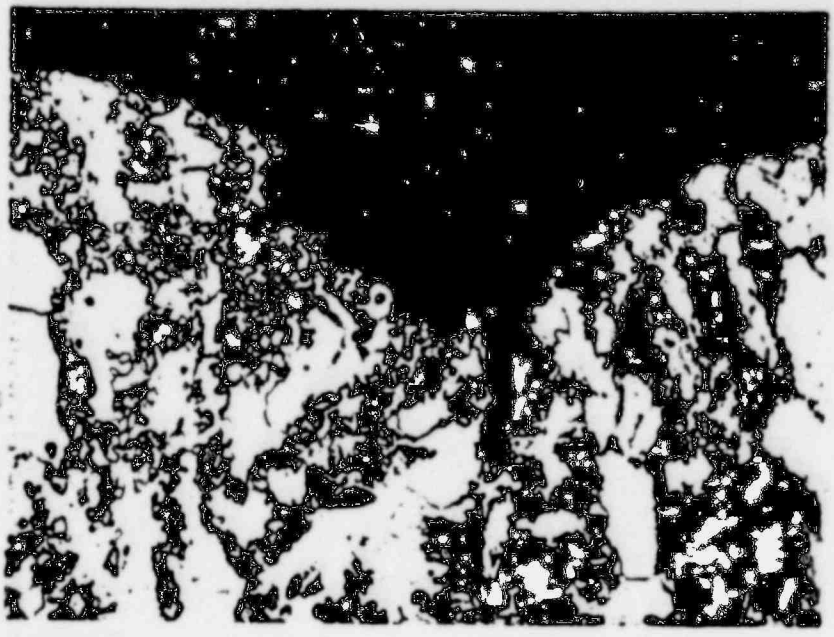

2-38112 500X

(a)

2-38113 300X

(b)

FIGURE 12. CRACKS DETECTED AT THE COUNTERBORE REGION AT THE 16-IN. REDUCER END.

2-37793 300X

(a)

2-37935 500X

(b)

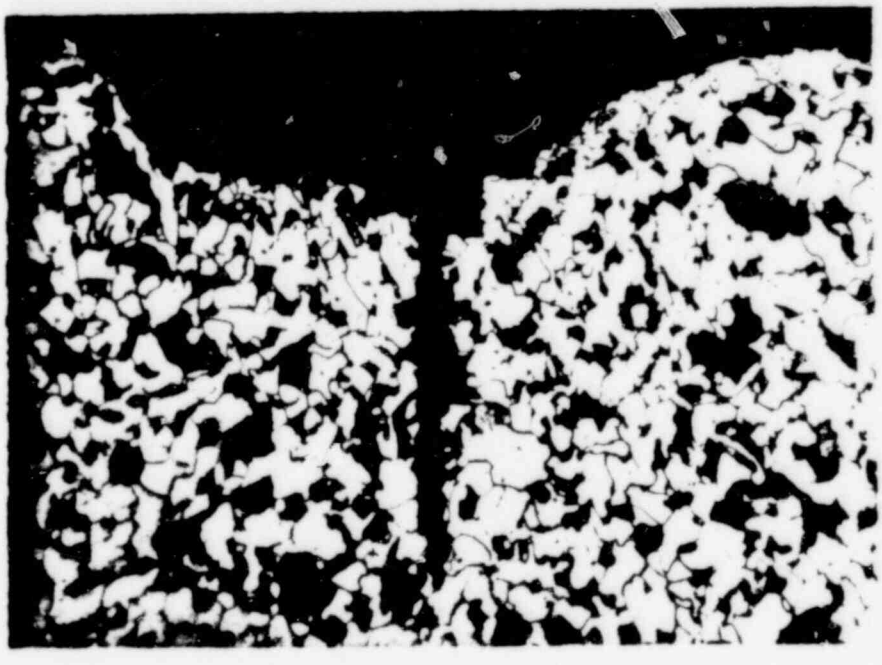

2-37796 300X

(c)

FIGURE 13. DETAILED VIEW OF TYPICAL CRACK TIPS, ETCHANT: NITAL. Sections taken at stations #19 [see Figure 5(b)], (a), and #34 of 18" reducer end and station #14, (b), of 16" reducer to pipe weld [see Figure 7(b)].

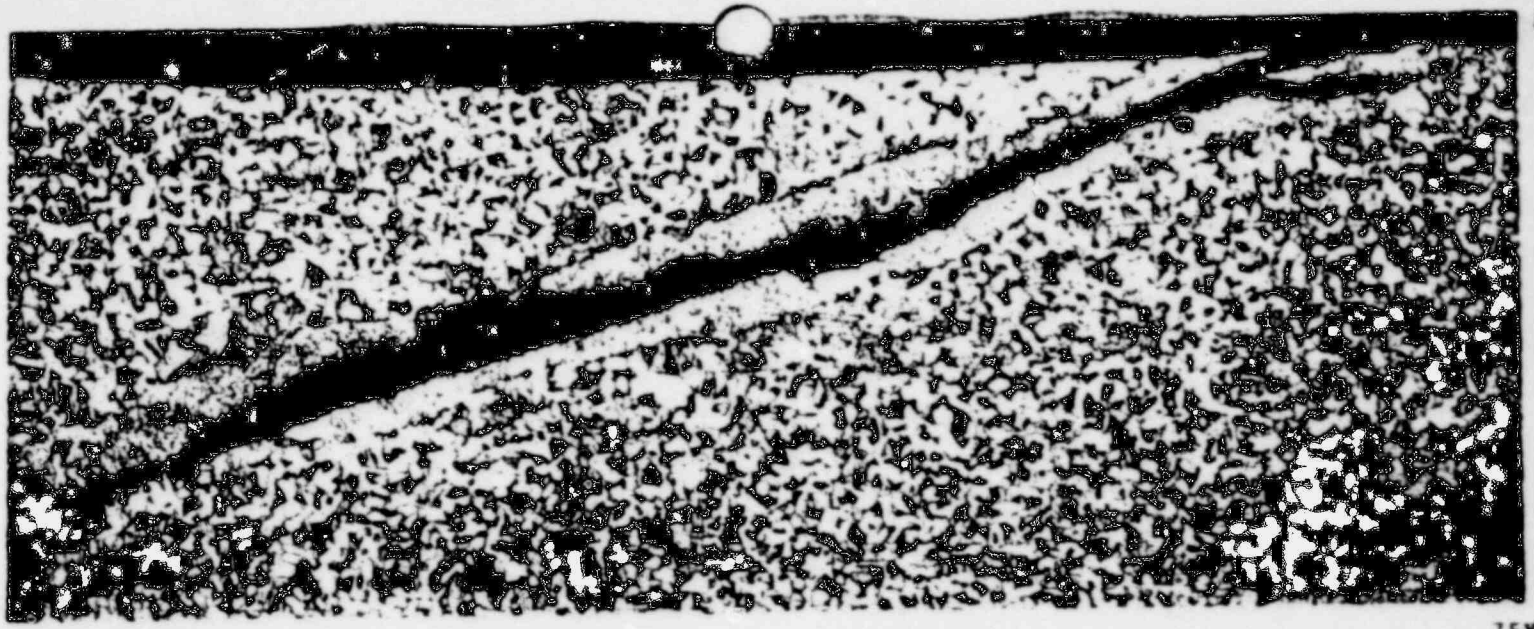

2-37864-65

75X

(a)

2-37863

300X

(b)

FIGURE 14. TRANSVERSE SECTION THROUGH CRACK AT O.D. Note the decarburized zone surrounding the oxide filled crack, (a), and the absence of a distinct interface, (b), between this zone and the base metal.

2-37620 4X

(a)

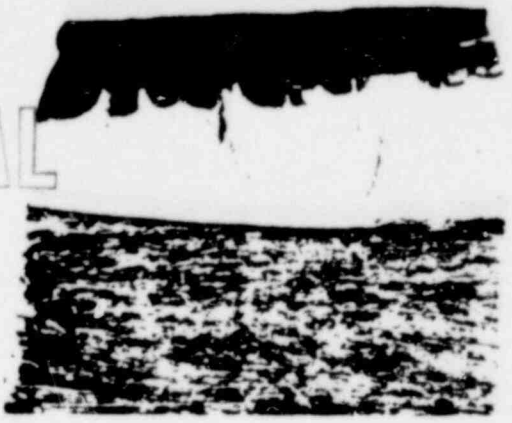

2-37619 4X

(b)

2-37619 12X

(c)

FIGURE 15. SAMPLES FROM STATION #15, (a) AND #43, (b) and (c), READY FOR FRACTOGRAPHIC EXAMINATION.

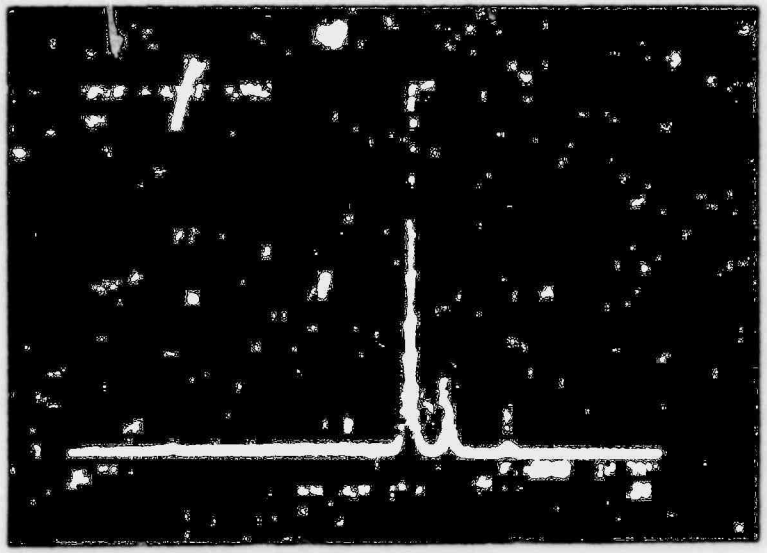

2-1949-S

(a)

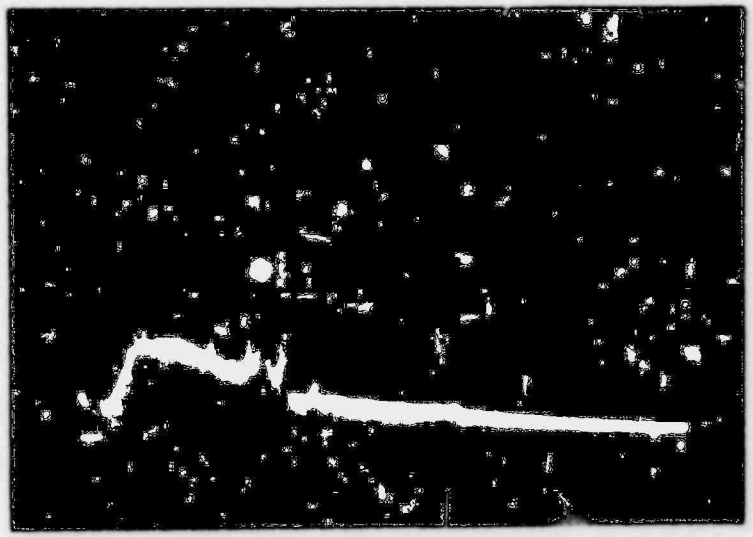

2-1978-S

(b)

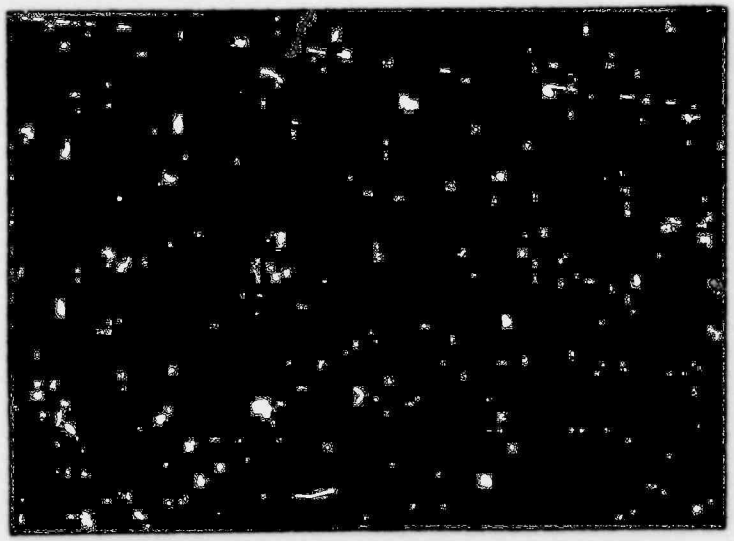

2-1979-S

(c)

FIGURE 17. TYPICAL ENERGY DISPERSIVE X-RAY SPECTRA. In-service crack surface, (a) and (b) and laboratory fracture surface, (c). Spectrum (b) has been expanded to show the low level leaks.

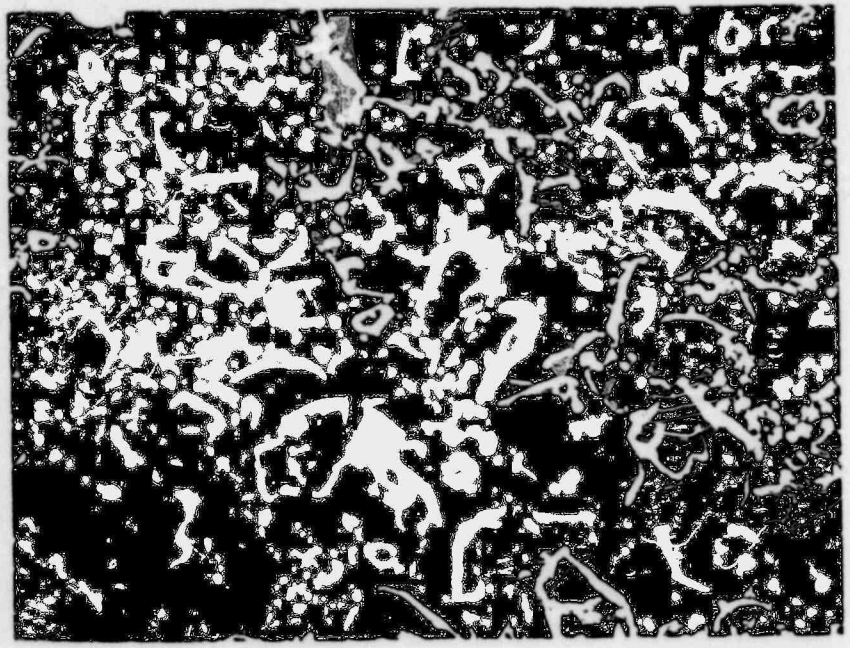

2-1948-S

500X

(a)

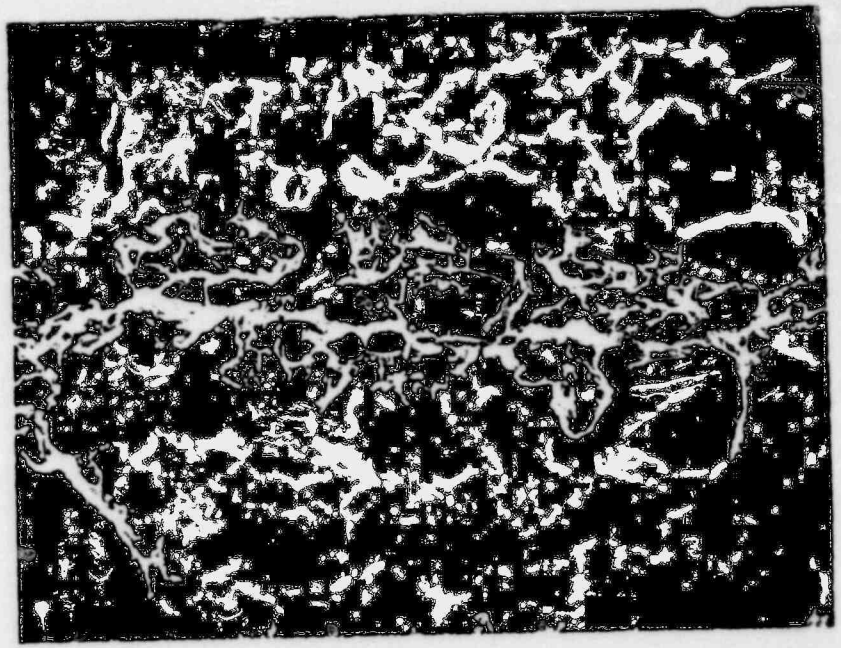

2-2067-S

200X

(b)

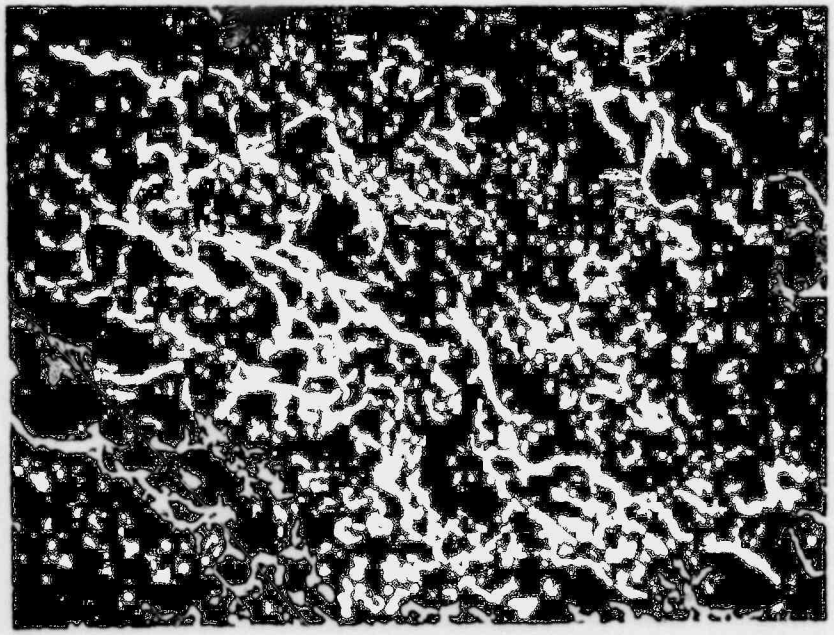

2-2083-S

1000X

FIGURE 16. TYPICAL FRACTURE SURFACES OF CRACKS IN 18-IN. REDUCER END, BEFORE OXIDE REMOVAL, (a) AND (b), AND AFTER OXIDE REMOVAL, (c).

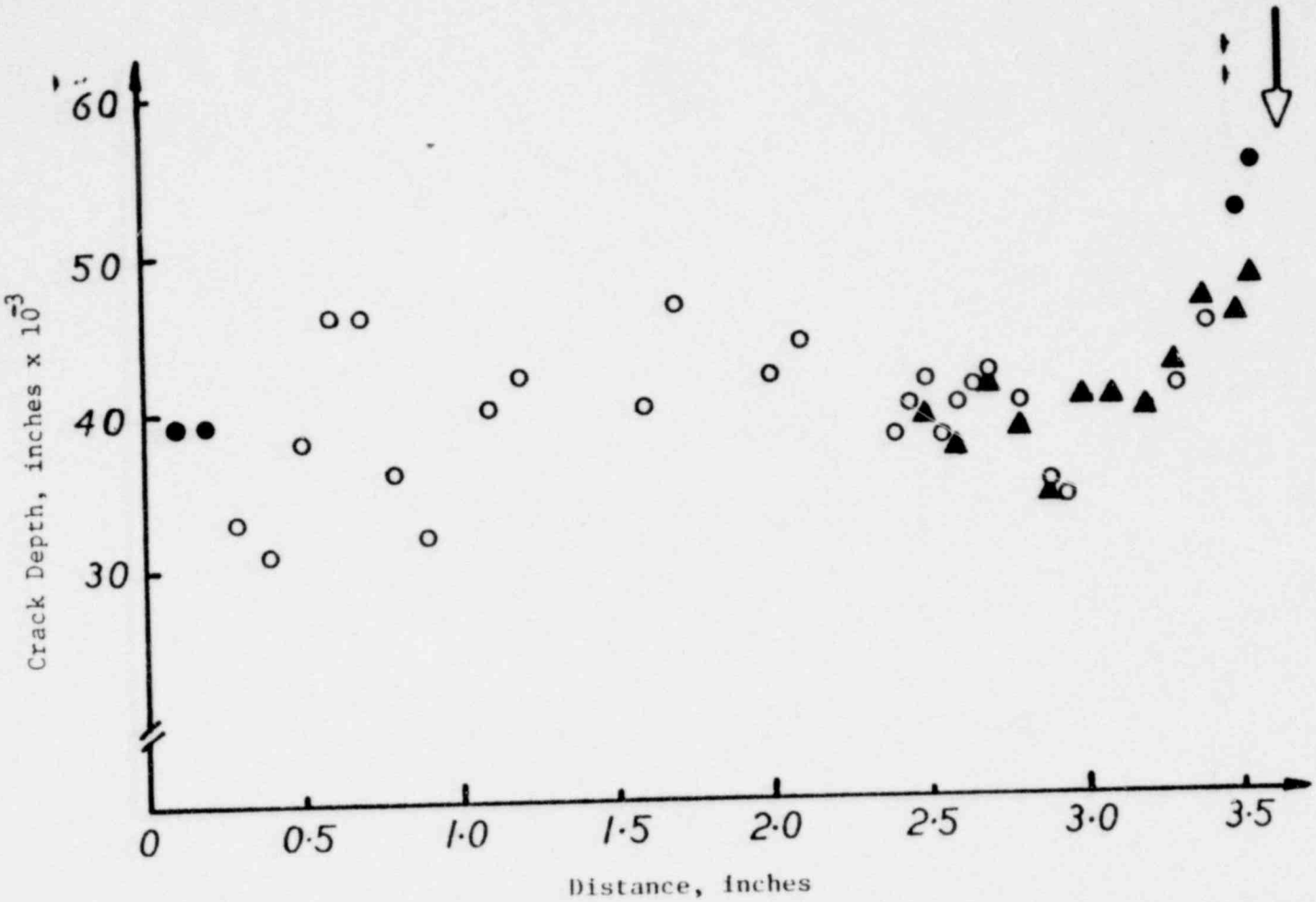

FIGURE 18. COMPARISON OF CRACK DEPTH MEASUREMENTS USING THE (NONDESTRUCTIVE) SATELLITE-PULSE TECHNIQUE, ○, AND (DESTRUCTIVE) DIRECT MEASUREMENT ▲ The solid circles are believed to have been influenced by edge effects. The edges of the sample were zero and 3.6 inches (marked by arrow).